Supporting information

Functionalized silica nanoplatform as a bimodal contrast agent for MRI and optical imaging

Sarah Garifo, [a] Dimitri Stanicki, [a] Sébastien Boutry, [b] Lionel Larbanoix, [b] Indiana Ternad, [a] Robert N. Muller, [a,b] and Sophie Laurent *[a,b]

[a.] General, Organic and Biomedical Chemistry Unit, NMR and Molecular Imaging Laboratory, University of Mons, 19 avenue Maistriau, 7000 Mons, Belgium. E-mail: sophie.laurent@umons.ac.be; Tel.: +32-(0)65-37-35-25

[b.] Center for Microscopy and Molecular Imaging (CMMI), 8 rue Adrienne Bolland, 6041 Gosselies, Belgium

- SiO_2-NPs surface modification

Figure S1 shows TEM images of the raw SiO_2-NPs formation with surface reactivation with TEOS and PEG-coated SiO_2-NPs (D^{TEM} = 28.26 ± 3.18 nm, PDI^{TEM}: 1.04).

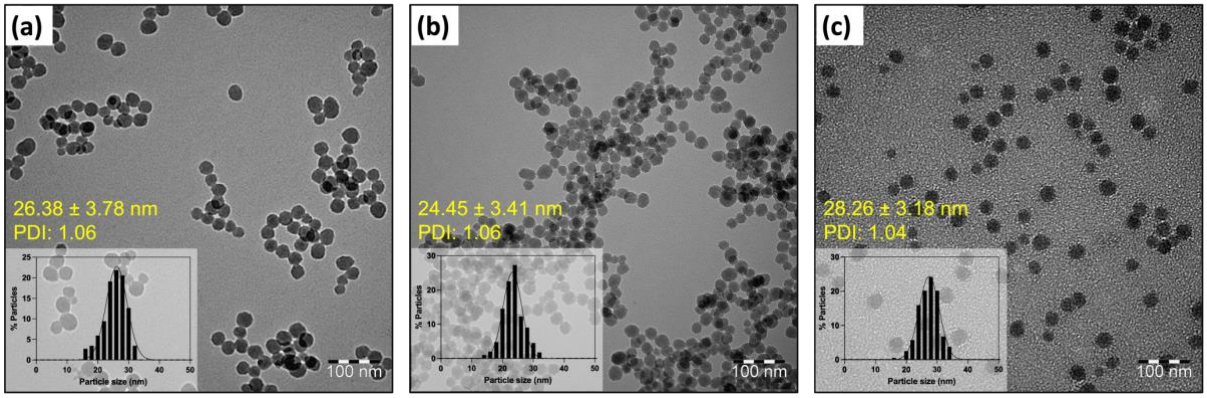

Fig. S1 Surface growth of empty NPs: **(a)** (growth step 1, day one), **(b)** surface reactivated (growth step 2, day two) and **(c)** PEG-coated NPs.

The scale bars correspond to 100 nm (93000-fold zoom). Insets show the TEM size distributions determined by statistical analysis. Average D^{TEM} diameters were estimated over multiple TEM images recorded for each triplicate.

The stability and hydrodynamic diameter were evaluated by PCS displaying a mean hydrodynamic diameter close to 110 nm for PEG-coated SiO_2-NPs (Fig. S2; D_H^{DLS}: 114 nm; PDI^{DLS}: 0.17).

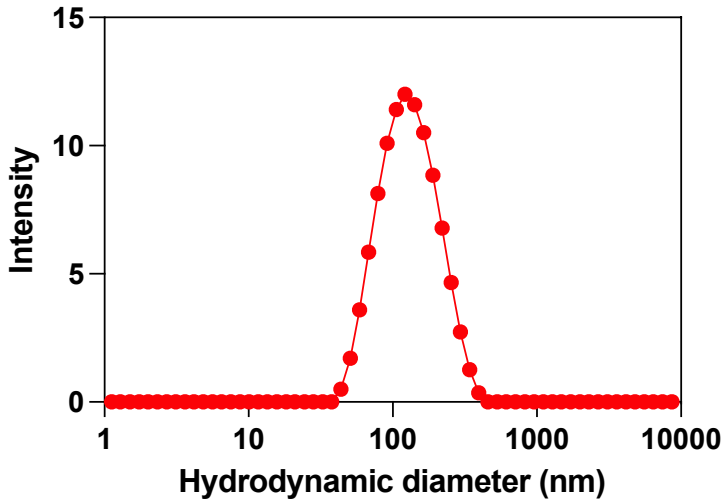

Fig. S2. Stability measurements by DLS on PEG-coated SiO_2-NPs (mean hydrodynamic diameter reached 114 nm (PDI: 0.17).

Thermogravimetric analyses (Fig. S3) were registered on empty PEG-coated SiO_2-NPs samples by detecting a weight loss of 18% attributable to the organic coating.

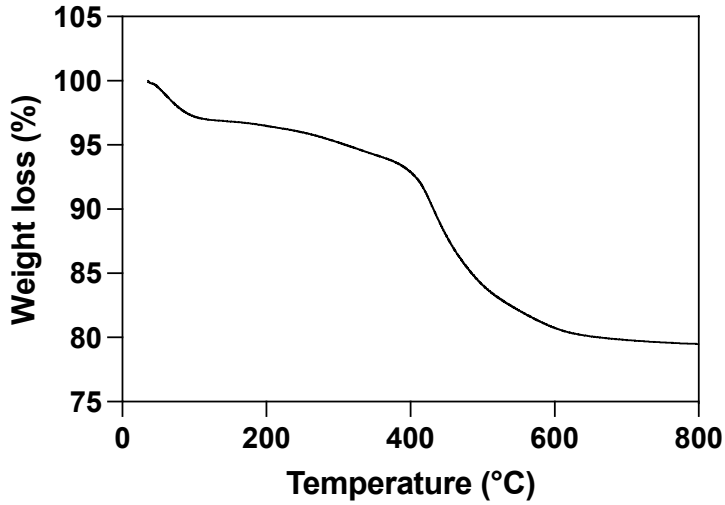

Fig. S3 Thermogravimetric (TGA) curve of empty PEG-coated SiO_2-NPs system.

The surface modification of silica nanoparticles was confirmed by FTIR (Fig. S4). The spectra following the PEGylation procedure exhibited the characteristic absorption bands for the polymer backbone groups as shown in Figure S4. First, the peaks specific to the different vibration modes of the SiO_2 network were observed at 1100, 960 and 790 cm^{-1} owing to Si-O-Si asymmetric stretching vibrations, Si-OH stretching and Si-O-Si symmetric stretching, respectively. The peak at 1660 cm^{-1} was attributed to the characteristic SiO-H bending of physisorbed water molecules.

After surface modification, the new absorption bands at 2870, 1460 and 1350 cm^{-1} were assigned to the stretching and bending of the C-H and C-O bonds from polymeric chains, respectively.

After 3*H*-DiazBA insertion onto the PEG corona surrounding SiO_2-NPs and purification steps, the resulted powder was characterized by IR spectroscopy. The C=O stretching band from carboxylic acid function was weak, appearing at 1710 cm^{-1} in the FTIR spectrum.

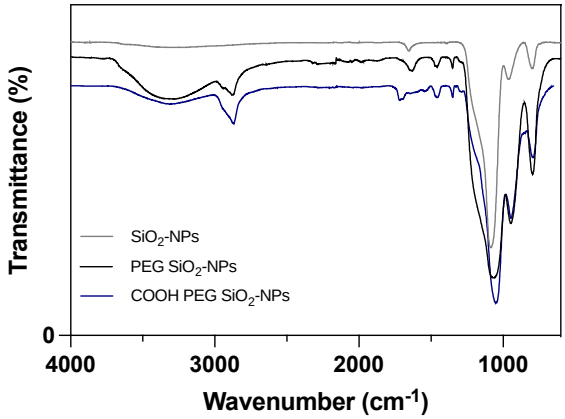

Fig. S4 Normalized FTIR spectra of SiO_2-NPs, PEG-coated SiO_2-NPs and functionalized NPs.

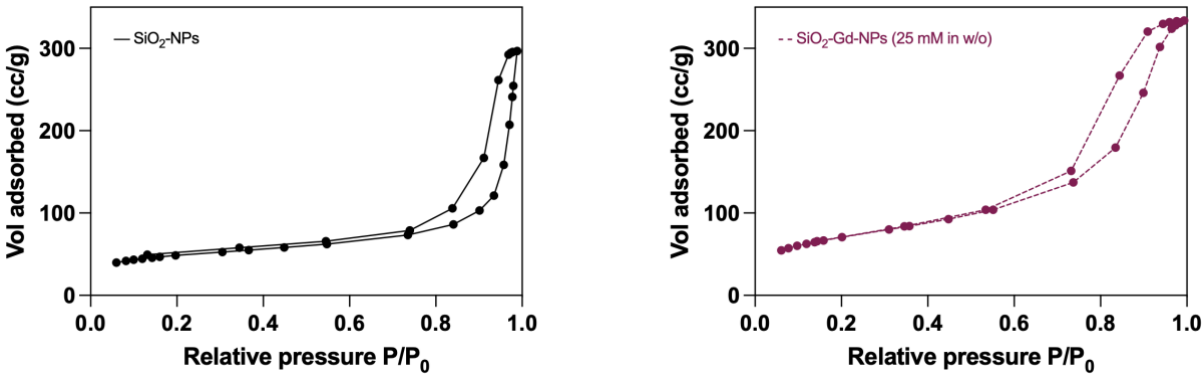

Fig. S5 BET experiments. Isotherms plot from absorption and desorption of nitrogen on empty SiO_2-NPs and on $NP^{16\ nm}Gd$ (25 mM in w/o step).

DLS measurements were performed before and after functionalization of SiO_2-NPs and assessed the stability of the suspensions in aqueous and physiological media (Fig. S6).

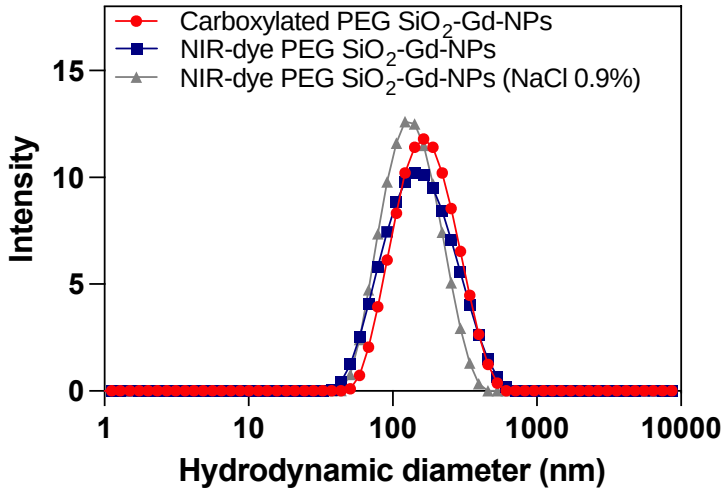

Fig. S6. Stability measurements by DLS.

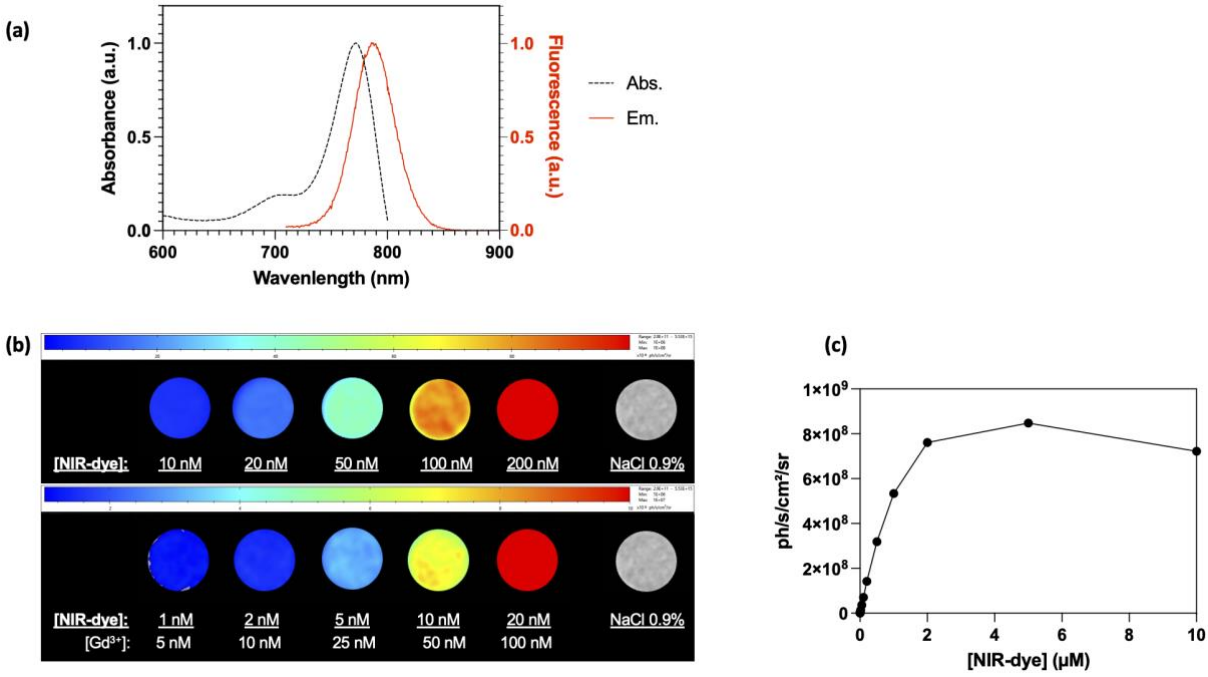

Fig. S7 Fluorescent properties of NIR-dye PEG-coated SiO_2-Gd-NPs. **(a)** Normalized NIR absorbance (Abs, dashed line) and emission (Em, solid line) spectrum of bimodal MRI/OI silica platform. **(b)** Phantom optical imaging (FLI) experiment of the silica probe from left to right, NaCl 0.9%, diluted suspensions of 1 nM to 200 nM of NIR-dye anchored on SiO_2-NPs ($\lambda_{excitation}$ = 687 nm, $\lambda_{emission}$ = 797 nm). **(c)** Signal intensities (photons s^{-1} cm^{-2} sr^{-1}) evolution.

- Number of Gd^{3+} complexes embedded inside silica NP

The mean number of complexes entrapped inside a nanoparticle in suspension (n_{cplx}) was approximated through the following experimental data: the NP radius as determined by TEM

microscopy (r_{NP}), the gadolinium concentration from ICP-AES analysis and the mass of silica (m) after drying 1 milliliter of colloidal suspension.

Considering the volume of a single spherical particle (eqn S1), the mass related to a single digit (eqn S2) and the density of the bulk material (ρ = 2.4 g cm^{-3} at 20°C), the mass of a single nanoparticle (m_{NP}) in suspension was estimated.

$$V_{NP} = \frac{4}{3}\,\pi\, r_{NP}^3 \qquad \text{(eqn S1)} \qquad m_{NP} = V_{NP}\,\rho \qquad \text{(eqn S2)}$$

The number of particles in the sample (n_{NP}) was derived from the following relation (eqn S3). Taking into account Avogadro number and Gd^{3+} concentration, the number of complexes per particle was obtained (eqn S4).

$$n_{NP} = \frac{m}{m_{NP}} \qquad \text{(eqn S3)} \qquad n_{cplx} = \frac{[Gd^{3+}]\,N_A}{n_{NP}} \qquad \text{(eqn S4)}$$

The numbers of encapsuled complexes according to the synthesis procedure are gathered in the table below (Table S1).

Table S1. Number of entrapped complexes inside SiO_2-NPs (average values of triplicate).

Systems	n_{cplx}
$NP^{16\ nm}Gd$	≈ 80 complexes/NP
$NP^{18\ nm}Gd$	≈ 130 complexes/NP
$NP^{25\ nm}Gd$	≈ 320 complexes/NP

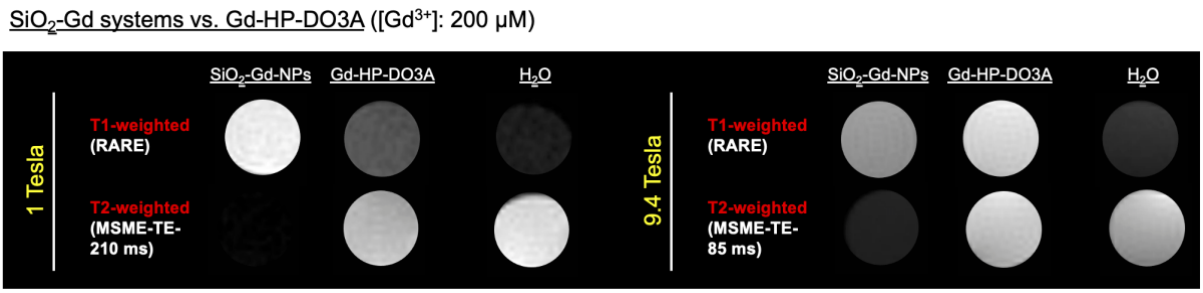

Fig. S8 SiO_2-Gd-NPs *vs.* free Gd-HP-DO3A (200 µM of gadolinium) *vs.* water, respectively from left, middle and right. Comparison of the signal enhancement/decease at 1 and 9.4 Tesla, T_1-W and T_2-W.

- Biodistribution studies

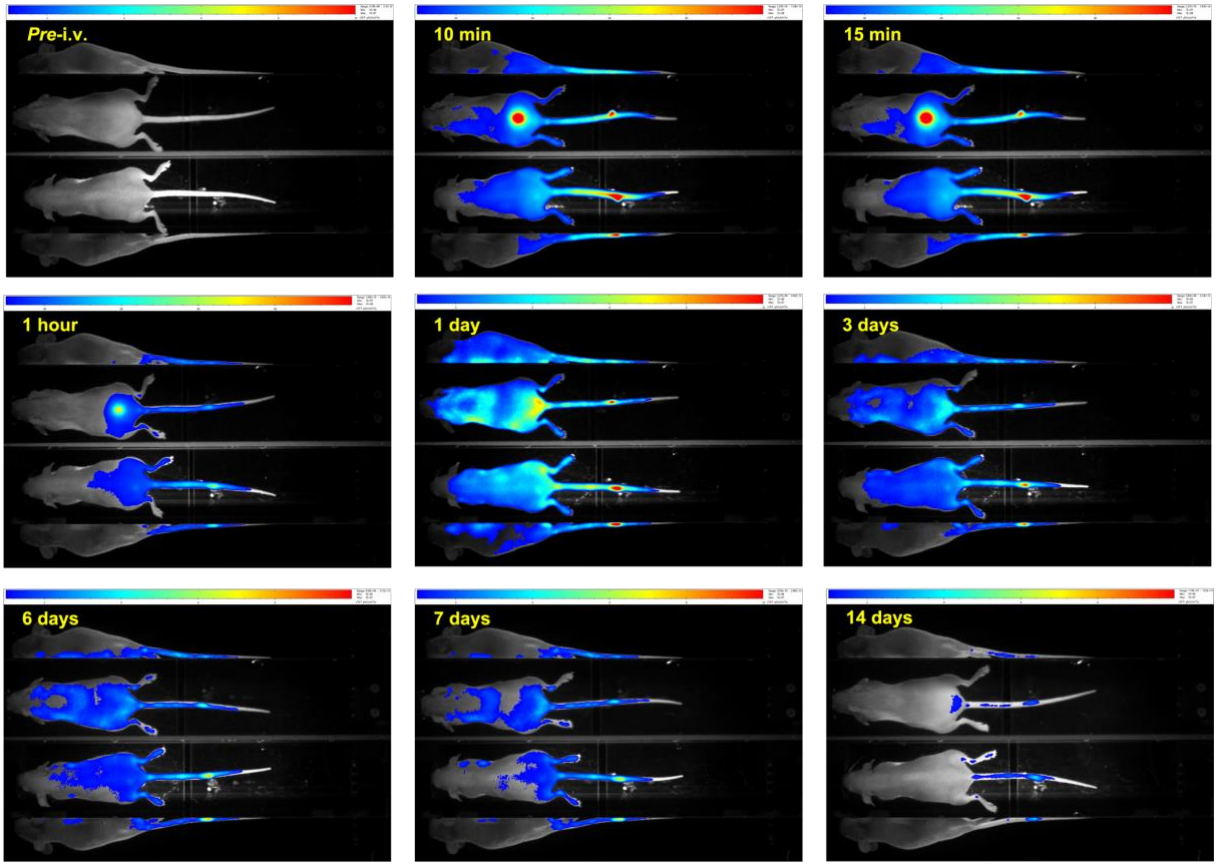

Fig. S9 *In vivo* FLI experiment with 4-views (right and left -lateral, ventral and dorsal) collection images collected on mice i.v. injected with NIR-dye PEG-coated SiO_2-Gd-NPs (10 mmol, 45 µL, 230 µM) from pre to 14 days post-injection.

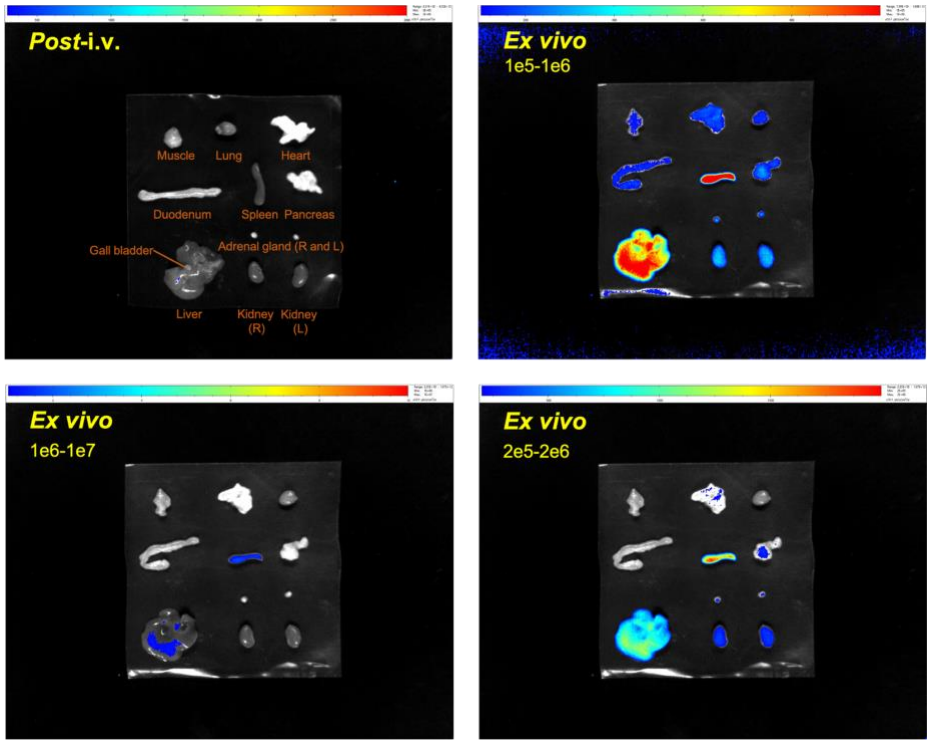

Fig. S10 *Ex vivo* FLI of organs of interest (after 14 days).

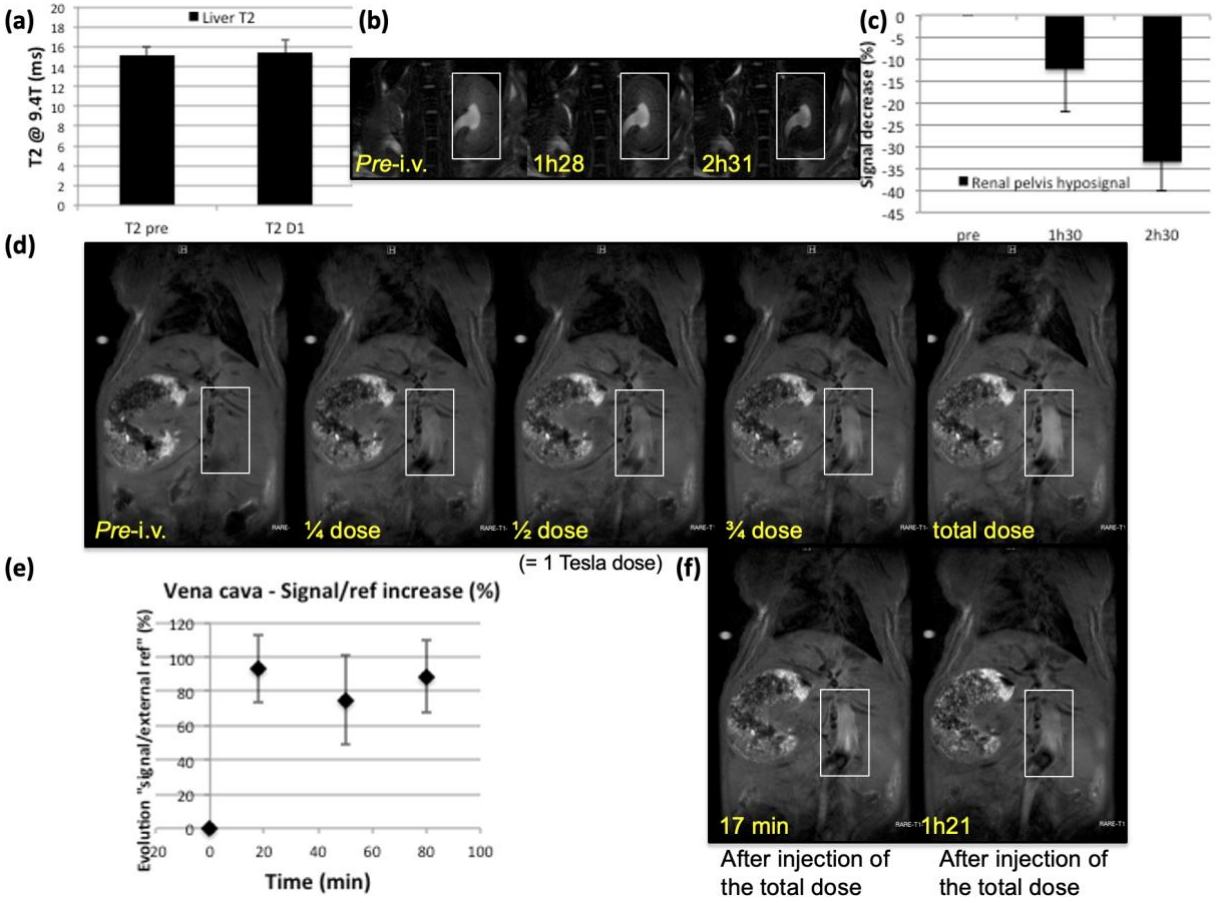

Fig. S11 (a-c) Analysis of negative signal enhancement at 9.4 T and representative T_2-weighted MR images before and up to 150 mins or day 1 after i.v. injection of NIR-dye PEG-SiO_2-Gd-NPs (signal enhancement data are quantified from measurements in ROIs in specific organs; as a T_2 value or as a signal intensity value represented as a percentage of the pre-injection value). **(a)** concerns the liver (n = 3) before and one day after injection of 4.3 µmoles Gd/kg; **(b)** and **(c)** concern renal pelvis (kidney surrounded by a white square) before and in first hours after injection of 8.6 µmoles Gd/kg (n = 2-3). Mean values +/- std deviation of the mean are represented on graphs. **(d)** and **(f)** Analysis of positive signal enhancement and 9.4 T representative T_1-weighted MR images before, in dose-related experiment, and during 80 mins after i.v. injection (black sign) of the total dose (8.6 µmoles Gd/kg) of NIR-dye PEG-SiO_2-Gd-NPs (signal enhancement data are normalized as a calculated ratio between respective signals in organs or vessel specific ROIs and in an external Gd-containing reference and represented as a percentage of the pre-injection value). **(d)**, **(e)** and **(f)** concern vena cava (surrounded by a white square); Mean values +/- std deviation of the mean are represented on graphs (n = 3).

- Preliminary photoacoustic (MSOT) experiments (phantoms)

Interestingly, as a complementary method for fluorescent probes, the phantoms imaging experiments were completed by PAI characterizations of the multimodal particles. The detection threshold reached 1.25 pmol of NIR-dye (0.3 µg of particles) on NIR-dye PEG-coated SiO_2-Gd-NPs (1 µM of NIR-dye) which suggested a particularly attractive use of the platform for MSOT tomography (Fig. S12).

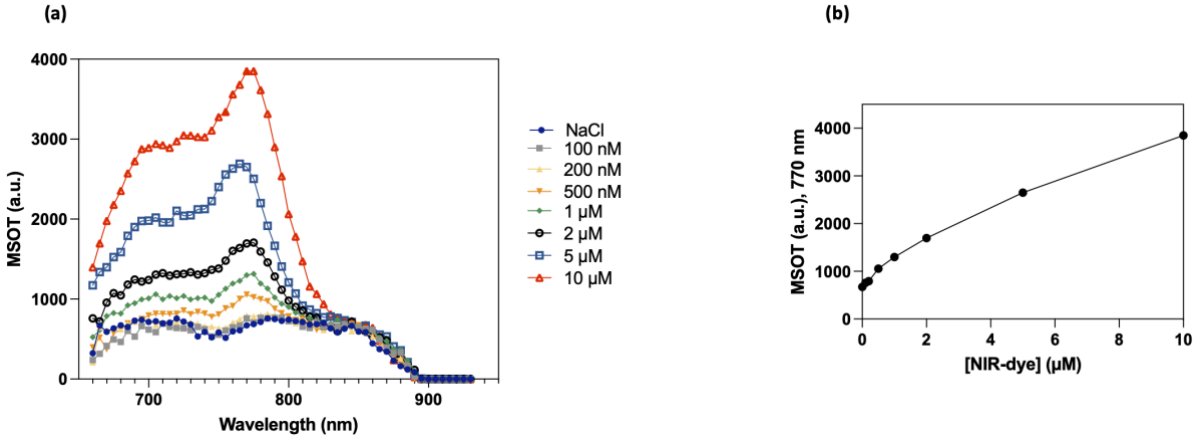

Fig. S12 Optoacoustic imaging experiments of NIR-dye PEG-coated SiO_2-Gd-NPs. **(a)** photoacoustic spectra recorded on phantom images of NIR-dye PEG-coated SiO_2-Gd-NPs at various concentrations and **(b)** evolution of MSOT signal (770 nm).